We are IntechOpen, the world's leading publisher of Open Access books Built by scientists, for scientists

4,800
Open access books available

122,000
International authors and editors

135M
Downloads

Our authors are among the

154
Countries delivered to

TOP 1%
most cited scientists

12.2%
Contributors from top 500 universities

CLARIVATE ANALYTICS BOOK CITATION INDEX INDEXED

WEB OF SCIENCE™

Selection of our books indexed in the Book Citation Index in Web of Science™ Core Collection (BKCI)

Interested in publishing with us?
Contact book.department@intechopen.com

Numbers displayed above are based on latest data collected.
For more information visit www.intechopen.com

10

Broad Applications of Multi-Colour Time-Resolved Flow Cytometry

Ben J. Gu and James S. Wiley
Florey Neuroscience Institutes, The University of Melbourne
Australia

1. Introduction

Flow cytometer has become an indispensable tool used in medical research. After 50 years' development, flow cytometry has been dramatically advanced in its capability and sensitivity. Different refinements of hardware and software have also been developed to accommodate the diverse applications in biomedicine, biology and chemistry. However, the basic principle is still the same: as fluorescent particles in suspension pass through one or more focused laser beams, their fluorescence emission signals are processed in real time (Sklar *et al.*, 2007). The intensity of emission signal is proportional to number of fluorescence molecules illuminated on the fluorescent particle. This feature also enables kinetic measurement of fluorescence changes over a certain period of time in a specific sub-population of particles in suspension, which is known as time-resolved flow cytometry (TR-FCM). Considering the speed and throughput of flow cytometry, TR-FCM is particular attractive in studying cellular process of molecule binding, uptake of dye and influx/efflux over a scale of seconds or minutes. Diverse applications are also applied in TR-FCM, including time-resolved fluorescence decay measurement using a pulsed laser (Condrau *et al.*, 1994a; Condrau *et al.*, 1994b), high-throughput high-content screening of air-bubble separated samples using the HyperCyt system (Edwards *et al.*, 2001b; Ramirez *et al.*, 2003), and most frequently, real-time cellular kinetics, such as Ca^{2+} influx, intracellular pH changes, cell morphology and ligand-receptor interactions. These broad applications make TR-FCM a powerful technique in discovery of cellular functions.

In this chapter, we will use studies of the P2X7 receptor as an example of the applications of TR-FCM in assessing this receptor's cellular functions in real-time. The P2X7 receptor has a ubiquitous distribution in nearly all tissues and organs of the body with the highest expression in immune cells of monocyte-macrophage origin. The receptor is present as a trimer and its activation by extracellular ATP opens a cationic channel which gradually dilates to a larger pore over tens of seconds. Activation of P2X7 is associated with massive K^+ efflux which is a cofactor for assembly of the NALP3 inflammasome and secretion of inflammatory interleukins from myeloid cells. Prolonged activation of P2X7 leads to apoptotic death of the cell. P2X7 also has a function in the absence of its ligand, namely the recognition and phagocytosis of foreign particles in the absence of opsonins (Gu *et al.*, 2010; Gu *et al.*, 2011), and these features suggest that P2X7 and its downstream signalling pathways are important in innate immunity.

1.1 Equipment required for kinetic flow cytometry

The state-of-art flow cytometry is capable of measuring up to 50,000 events per second. For kinetic flow cytometry, events are accumulated and averaged over successive time intervals, typically 1 to 10 seconds or longer. Most kinetic studies require addition of an agonist or probe either to start or during the run, which may take 2 to 5 seconds. This time limitation has prevented the use of kinetic flow cytometry in studying rapid molecular interactions occurring on a time frame of less than one second. Over the last few decades, a number of on-line injection/mixing devices have been developed to reduce the dead-time to less than one second. One of these devices is the stopped-flow and coaxial mixing (Nolan & Sklar, 1998), another commercially available device is the Time Zero system produced by Cytek (http://www.cytekdev.com/pages/Accessories.html). This device allows precise temperature control and stirring of cells suspension to which a stimulus (agonist) is delivered within one second, allowing uninterrupted measurement of cellular response.

Fig. 1. A picture of Time Zero module integrated with a FACSCalibur flow cytometer

This Time Zero system is compatible with almost all the BD flow cytometers, as well as old models of Coulter flow cytometer (EPICS, Elite). It consists of two modules, the Time Zero module with water-jacket tube holder and the Air Supply module. An additional circulating water bath is also needed if temperature control is required. To install this device, the Air Supply module has to be connected to the air pressure system of the flow cytometer via a three-way valve, the sample nozzle has to be connected with a soft tubing and the short tubes (2.5 mL) have to be used instead of regular 5 mL FACS tubes. These changes may take 10-15 min to setup and another 10-15 min to clean up after each run. Since most flow cytometers are shared core facilities, other users may be affected by these changes. If subsecond cell response is not crucial for the study, an alternative way is to unscrew the sample platform (takes about 10 seconds) and fit the water-jacket tube holder on the sample bar of a BD flow cytometer (Fig. 1). The Air Supply module is therefore not

needed, and regular 5 mL tubes can be used. However, the tube has to be physically removed and replaced after the addition of stimulus, which incurs a delay of 2-5 seconds before recording. In either case, a tiny stir bar (1x3 mm) has to be placed in the bottom of tube in order to mix cells. A major advantage of the Time Zero system is the device for magnetic stirring of the reaction cuvette, which maximizes the number of cell-cell interactions as well as rapidly mixing agonist or probe into the suspension. It is also a good idea to leave a small amount of water inside the water-jacket tube holder to ensure good thermal conductivity to the tube.

1.2 Quantitation of the kinetic response of cells

The two methods used to quantitate the kinetic response are either slope of a curve or area under a curve. In general, slope of a curve is more appropriate for rapid linear responses while area under a curve is more accurate for non-linear responses. Since most cellular responses are the results of multiple driving forces, and variations between each intervals are often seen in flow cytometry, area under a curve may be a better way to describe the quantitative information given by kinetic flow cytometry.

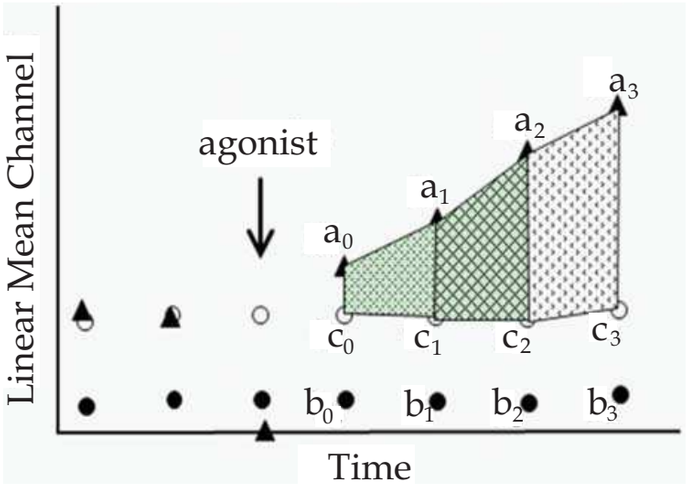

Fig. 2. A schematic illustration of area under a curve

To quantify dye uptake, arbitrary units of area under a curve in a certain time period (a number of time intervals, n*Δt) after addition of stimulus is calculated (Fig. 2). The basal line (without stimulus) has to be adjusted to the same level as the test line (with stimulus added). The area under a curve between the basal and test lines is considered as the sum of n trapezoids (Fig. 2). Therefore, the following mathematical model based on the trapezoid rule is used for the area calculation:

a_0,a_1…a_n are the linear mean channel values of each interval from the ATP-induced ethidium uptake curve while b_0,b_1…b_{60} are those from the basal line, and c_0,c_1…c_{60} are those from the adjusted basal line. Therefore,

Area(1)=0.5 x (a_0-c_0+a_1-c_1) x Δt
Area(2)=0.5 x (a_1-c_1+a_2-c_2) x Δt
Area(n)=0.5 x (a_{n-1}-c_{n-1}+a_n-c_n) x Δt

Area=0.5 x Δt x **(**sum(a_0,a_1,…a_{n-1})+sum(a_1,a_2,…a_n)
-sum(c_0,c_1,..c_{n-1})-sum(c_1,c_2,..c_{60})**)**
as c = b + Δb
$\therefore$ Area = 0.5 x Δt x **(** sum(a_0,a_1,…a_n)+sum(a_1,a_2,…a_n)
-(sum(b_0,b_1,..b_n)-(sum(b_1,b_2,..b_n)-2x n x Δb)**)**

The area under a curve can then be calculated using a Microsoft Excel function.

1.3 Software for kinetic flow cytometry

Not many programs are available to process kinetic data from flow cytometry. The best freeware is WinMDI, written by Joseph Trotter of The Scripps Research Institute, La Jolla, CA 92037. The latest version of this freeware can be downloaded from http://facs.scripps.edu/software.html. WinMDI is able to calculate the mean fluorescence intensity (MFI) between defined time intervals. The data can be saved as a Tab separated text file which can then be imported by Microsoft Excel. However, WinMDI was originally written for Windows 3, and has not been updated. It can only read FCS 2.0 file, and does not recognize long file names. A brief tutorial for WinMDI by Dr Gérald Grégori can be found at http://www.cyto.purdue.edu/archive/flowcyt/labinfo/images/TutorialWinMDI.pdf. A more advanced program is FlowJo from the Tree Star Inc. Its kinetic tool can not only calculate MFI over time intervals, but also give both slope and area under the curve. The detailed instruction on the kinetic tool can be found at http://www.flowjo.com/home/tutorials/kinetics.html. Despite a number of bugs in this software, it can read FCS 3.0 file (a file format used by all latest flow cytometers) and is compatible with both Mac OS and Windows. Another software called Cyflogic (http://www.cyflogic.fi/) also includes a kinetic tool (flux trace) in its licensed version (not the free non-commercial version). Cyflogic has a similar interface as WinMDI, and can also recognize FCS 3.0 files.

In the following sections, we will use WinMDI to demonstrate how the kinetic flow cytometry analysis is performed. To use it, first choose "Display|Density Plot" on the menu, select the file, in the popup window "Format 2D Display", choose "256x256" for "Display Array Resolution" which gives a better resolution. Left click on the density plot, choose "Regions" to create a polygon gate R1 based on Forward Scatter & Side Scatter. Then choose "Display|Dot Plot" to draw a dot plot of cell marker (e.g. CD14) versus main fluorescence (e.g. Fura-red, ethidium, or YG). On "Format Dotplot" window, choose "All" for "Plot number of events". Left click on the dot plot, choose "Regions" to create a "SortRect" gate R2 based on the cell marker and main fluorescence. After the two gates are set, draw another dot plot of time versus main fluorescence. On "Format Dotplot" window, choose "All" for "Plot number of events", and check "Kinetics mode", "Overlay kinetics line" and "Draw kinetics only" to draw a kinetics line in the dot plot (KinPlot). Left click on the plot, choose "Gates", select "And" for both R1 and R2. Choose the KinPlot window, then choose "File|Save as" to save the date to a tabed text file. The file can then be imported by Microsoft Excel.

2. $Ca^{2+/}Ba^{2+}$ influx with Fura-Red

2.1 Principles

Calcium influx/efflux is one of the most important cellular processes driven by opening of ion channels/receptors, including the P2X7 receptor. Following activation by extracellular

ATP, the P2X7 receptor opens a non-selective cation channel to allow Ca^{2+} influx and K^+ efflux. Many methods have been developed to measure P2X7 function by monitoring the cation flux through the open channel upon receptor activation. The most common ones are electrophysiological methods (patch-clamp and intracellular microelectrode), which are widely used in all receptor studies. Fluxes of divalent cations such as Ca^{2+}, Ba^{2+} as well as monovalent cations such as Rb^+, Na^+ and Li^+, have been used to study P2X7 channel function either by fluorometry with Fura-2 or with isotopes of these cations. However, interpretation of ionic flux methods requires a homogeneous cell population, while flow cytometric methods are applicable to mixed cell populations. We have developed a time-resolved flow cytometry method to monitor the influx of Ca^{2+} or Ba^{2+} into cells loaded with a fluorescent chelator, Fura-Red. Fura-Red is a fluorescent Ca^{2+} indicator which is excited by a standard argon laser (488 nm) and with emission at long wavelengths (~660 nm). This permits multi-colour analysis of Fura-Red signals in cells tagged with FITC-labelled antibodies using flow cytometry, allowing measurement of P2X7 function in specific cell types in a mixed cell population. Unlike the other fluorescent Ca^{2+} indicators, fluorescence of Fura-Red excited at 488 nm decreases once the indicator binds divalent cations such as Ca^{2+} or Ba^{2+} (Gu *et al.*, 2001; Jursik *et al.*, 2007).

2.2 Method

To study the Ba2+ influx following activation of P2X7 by ATP, mononuclear cells ($2x10^6$) are incubated in Ca^{2+} free Na medium (145 mM NaCl, 5 mM KCl, 10 mM Hepes, pH 7.5, supplemented with 0.1% BSA and 5mM glucose) with Fura-Red acetoxymethyl ester (1 µg/mL) for 30 min at 37°C. Cells are then washed twice with Na medium (with 1 mM Ca^{2+}) and labelled with FITC-conjugated cell markers for 15 min (CD14 for monocytes, CD19 for B-lymphocytes, CD3 for T-lymphocytes or CD56 for NK cells). These mononuclear cells are washed once and resuspended in K medium (150 mM KCl, 10 mM Hepes, pH 7.5, supplemented with 0.1% BSA and 5mM glucose) with 1 mM Ba^{2+} at 37°C. A small magnetic stir bar (1x3 mm) is added to the tube before it is inserted into the Time-Zero System. The FL3 voltage is adjusted to give a linear mean channel fluorescence intensity of ~700 for the gated population. No compensation is required between FL1 and FL3. ATP is added 40 sec later. Signals from mononuclear cells are acquired at about 2000 events per second on a Becton Dickinson FACSCalibur flow cytometer and the data comprising forward scatter (log mode), side scatter (log mode), FL1 (log mode), FL3 (linear mode, 1024 channels) and time (2 sec intervals) for each event are collected. Digitonin is added at the end of the run to estimate maximum values for Ca^{2+} influx. The data from each run (about 250 sec) is saved into a listmode file.

2.3 Gating and calculation

The listmode file is analysed by WinMDI. Cells are gated by forward and side scatter and by cell type specific antibodies. The linear mean channel of fluorescence intensity (1024 channels resolution) for each gated subpopulation (Fig. 4) over successive 2 sec intervals is plotted against time and saved into a text file.

The text file is then imported into *Microsoft* Excel, and the arbitrary units of area above the Ba^{2+} influx curve in 20 sec after addition of ATP is calculated using the following functions:

Function(C5) =AVERAGE(C$7:INDIRECT(ADDRESS(D4+5,COLUMN(),4,1),1))
(to calculate the average linear mean channel of basal line in the same period before ATP is added into the test tube)

Function(D4) =MATCH(0,D$7:D$50,0)
(to locate in which interval that ATP is added)

Function(D5) =AVERAGE(D$7:INDIRECT(ADDRESS(D4+5,COLUMN(),4,1),1))
(to calculate the average linear mean channel of basal line before ATP is added)

Function(D6) =(SUM(INDIRECT(ADDRESS(D4+10,COLUMN()-1,4,1),1):INDIRECT(ADDRESS(D4+21,COLUMN()-1,4,1),1))+(D5-C5)*10)+(SUM(INDIRECT(ADDRESS(D4+11,COLUMN()-1,4,1),1):INDIRECT(ADDRESS(D4+20,COLUMN()-1,4,1),1))+(D5-C5)*8)-SUM(INDIRECT(ADDRESS(D4+10,COLUMN(),4,1),1):INDIRECT(ADDRESS(D4+21,COLUMN(),4,1),1))-SUM(INDIRECT(ADDRESS(D4+11,COLUMN(),4,1),1):INDIRECT(ADDRESS(D4+20,COLUMN(),4,1),1))
(to calculate the first 20 sec area above Ba^{2+} influx curve after addition of ATP)

The arbitrary unit of area obtained in Function(D6) is also used to quantify the P2X7 channel function. (Excel template is available)

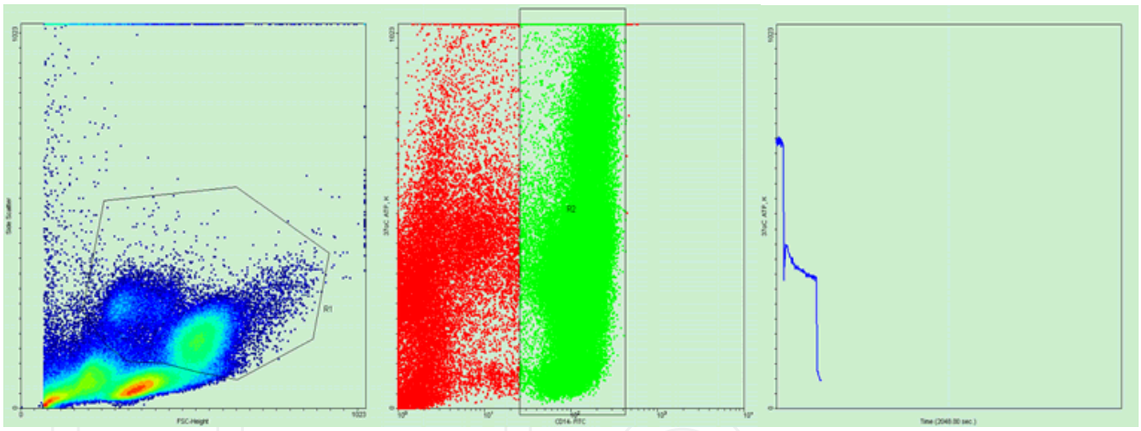

Fig. 4. Typical dotplots and gating strategy used to analyse Ba^{2+} influx by Fura-Red in CD14 positive monocytes

2.4 Notes for technique

Cation influx methods based on Fura-red fluorescence can be applied to kinetic studies in many channels/receptors which involve Ca^{2+} influx or efflux. In this study, Ba^{2+} is used as a surrogate for Ca^{2+} since cytosolic Ba^{2+} is neither pumped nor sequestered and the Ba^{2+} signal over short times represents the unidirectional influx. Most of the intracellular Ba^{2+} remains in the cytoplasmic region as mononuclear cells lack the mechanisms either to pump out intracellular Ba^{2+} or sequester this cation into intracellular organelles. Since P2X7 function is greater in Na^{+} free and/or Cl^{-} free buffer (Humphreys & Dubyak, 1996; Wiley *et al.*, 1992), isotonic K^{+} buffer is used to measure P2X7 function instead of physiological Na^{+} buffer.

In measurements of Ba^{2+} influx using Fura-red, because of the long wavelength emission of Fura-Red, there is little overlap between FL1 and FL3, and the FL3-FL1 compensation setting can be ignored. This long wavelength of Fura-Red also limits the interference of yellow coloured compounds.

	A	B	C	D
1				
2		Time (min)	Basal	ATP
3				
4			2s, 20s	21
5			693.59	708.24
6				5931
7	0	0	698.8	717.8
8	1	0.033333	708.1	706.2
9	2	0.066667	696.9	715.6
10	3	0.1	689	694.9
11	4	0.133333	706.3	708.6
12	5	0.166667	690.9	715.4
13	6	0.2	687.8	702.4
14	7	0.233333	697.1	723.6
15	8	0.266667	699.7	702.3
16	9	0.3	695.1	711.3
17	10	0.333333	707.8	711.3
18	11	0.366667	692.7	711.7
19	12	0.4	686.4	716.6
20	13	0.433333	681.8	702.8
21	14	0.466667	687.1	705.4
22	15	0.5	687.2	694
23	16	0.533333	697.6	712.8
24	17	0.566667	691.3	703.5
25	18	0.6	682.5	706.6
26	19	0.633333	687.6	702
27	20	0.666667	687.5	0
28	21	0.7	702	0
29	22	0.733333	684.5	0
30	23	0.766667	690	339.7
31	24	0.8	674.2	379
32	25	0.833333	683.2	393.3

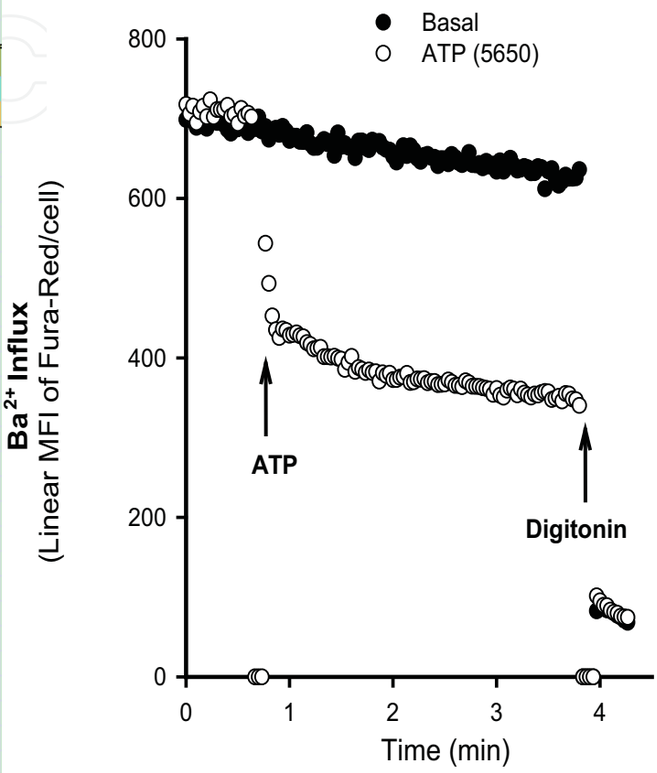

Fig. 5. An example of spreadsheet (left) and a typical curve of Ba^{2+} influx into cells (right)

3. ATP induced ethidium^{+} uptake

3.1 Principles

A unique feature of the P2X7 receptor observed under physiological conditions is the slow further increase in permeability that develops after the initial opening of the P2X7 channel, which is readily studied by flow cytometry (Wiley *et al.*, 1998). Ethidium bromide is a phenanthridinium intercalator which binds both DNA and RNA and is generally excluded from viable cells. It has been used previously to assess cell permeabilization by ATP (Gomperts, 1983). Once bound to nucleic acids, the fluorescence is enhanced 20~30 fold. The excitation maximum is shifted to 512 nm and the emission maximum is shifted to 605 nm. This long emission wavelength allows simultaneous detection of ethidium^{+} influx on the FL2 photomultiplier (570 to 610 nm) in the presence of FITC-labeled antibodies which are detected on the FL1 photomultiplier (525 nm). Time-resolved flow cytometry generates the mean fluorescence intensity of analysed cells over a certain time period. This technique

allows a sensitive measurement of the initial rate of ethidium uptake, which is essentially unidirectional because of binding of this permeant cation to nucleic acids. By using time-resolved flow cytometry, our group has shown that there is large variation of P2X7 function among individuals (Gu *et al.*, 2000) mainly due to genetic polymorphisms which alter the function of this receptor (Gu *et al.*, 2004; Gu *et al.*, 2001; Shemon *et al.*, 2006; Skarratt *et al.*, 2005; Wiley *et al.*, 2003)

Previous methods used to measure surface P2X7 function have been semi-quantitative and unable to distinguish sub-populations within the overall cell suspension as well as being unable to distinguish live and dead cells. The two-colour time resolved flow cytometry methods described here allow quantitative assessment of the abundance of functional P2X7 receptors on the surface of different subtypes of leukocytes as well as excluding dead cells from analysis (Gu *et al.*, 2000; Jursik *et al.*, 2007).

3.2 Method

Mononuclear cells ($2x10^6$) pre-labeled with FITC-conjugated cell markers are washed once and resuspended in 100 µL Na medium with 0.1 mM Ca^{2+} at room temperature. Following the addition of 900 µL K medium, a small magnetic stir bar is added to the tube before it is inserted into the Time-Zero System which controls temperature and allows magnetic stirring. The FL2 voltage is set at around 595V with a gain of 5.0, at which the linear mean channel fluorescence intensity for Quantum PE standard beads with MESF 300747 is 48±1 (256 linear scale) and the peak channel for right reference standard PE high level beads (MESF ~560,000) is 100±1 (256 linear scale). The compensation of FL1-FL2 and FL2-FL1 is 7% and 8% respectively. Ethidium bromide (25 µM) is added, followed 40 s later by addition of 1.0 mM ATP. Mononuclear cells are acquired at approximately 1000 events per second by a Becton Dickinson FACSCalibur flow cytometer and the data comprising forward scatter (log mode), side scatter (log mode), FL1 (log mode), FL2 (linear mode, 256 channels) and time (5 sec intervals) for each event are collected. The data of each run (approximately 380 sec) is saved into a listmode file.

3.3 Gating and calculation

The listmode file is analysed by WinMDI. Cells are gated by forward and side scatter and by cell type specific antibodies (Fig. 6). Cells with maximum ethidium$^+$ uptake (254 channels or over) are considered as fully permeable necrotic cells and therefore excluded from the assay. The kinetic linear mean channel of fluorescence intensity for each gated subpopulation over successive 5 sec intervals is plotted against time and saved into a text file.

To quantify ethidium$^+$ uptake, arbitrary unit of area under the uptake curve in the first 5 min after addition of ATP is calculated. The basal line (without ATP) is firstly adjusted to the same level as the test line (with ATP added after 40 sec). The area under the ethidium uptake curve between the basal and test lines is considered as the sum of 60 trapezoids (Fig. 1a).

The text file is then imported into *Microsoft* Excel, and the area under the ethidium$^+$ uptake curve is calculated using the following functions:

Function(C5)=AVERAGE(C$7:INDIRECT(ADDRESS(D4+5,COLUMN(),4,1),1))
(to calculate the average linear mean channel of basal line in the same period before ATP is added into the test tube)

Function(D4) =MATCH(0,D$7:D$30,0)
(to locate in which interval that ATP is added)

Function(D5) =AVERAGE(D$7:INDIRECT(ADDRESS(D4+5,COLUMN(),4,1),1))
(to calculate the average linear mean channel of basal line before ATP is added)

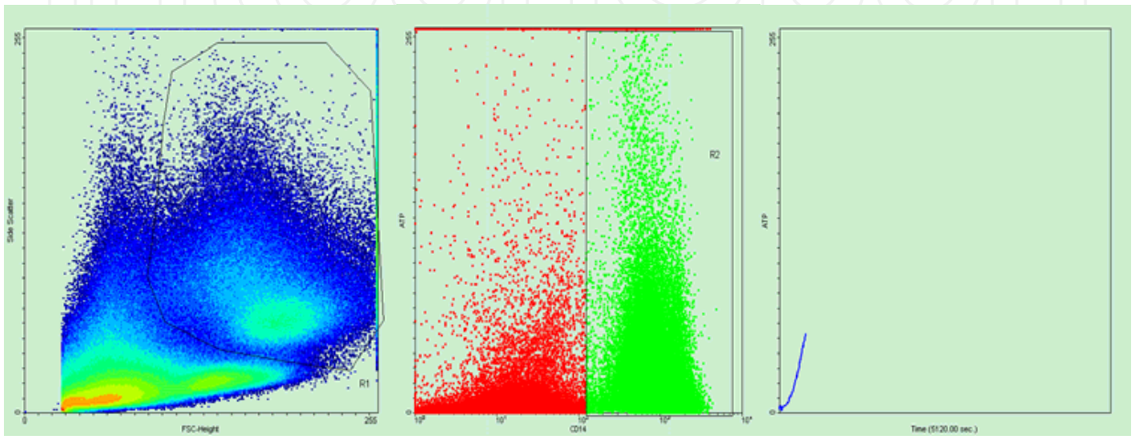

Fig. 6. Typical dotplots and gating strategy used to analyse ethidium$^+$ uptake by CD14 positive monocytes

	A	B	C	D	E
1					
2					
3		Time (min)	CD14 basal	CD14 ATP	
4			5s	6	3221
5			1.74	1.66	8654
6				26278	16871
7	0	0	1.5	1.5	
8	1	0.083333	1.9	1.3	
9	2	0.166667	2.1	1.7	
10	3	0.25	2	2.2	
11	4	0.333333	1.2	1.6	
12	5	0.416667	1	0	
13	6	0.5	1.9	2	
14	7	0.583333	1.5	3.3	
15	8	0.666667	2.2	3.8	
16	9	0.75	1.8	5.8	
17	10	0.833333	2.4	7.2	
18	11	0.916667	2	9.4	
19	12	1	2.1	11	
20	13	1.083333	2.5	12.8	
21	14	1.166667	2.3	15.8	
22	15	1.25	2.5	16.6	
23	16	1.333333	2.9	18.7	

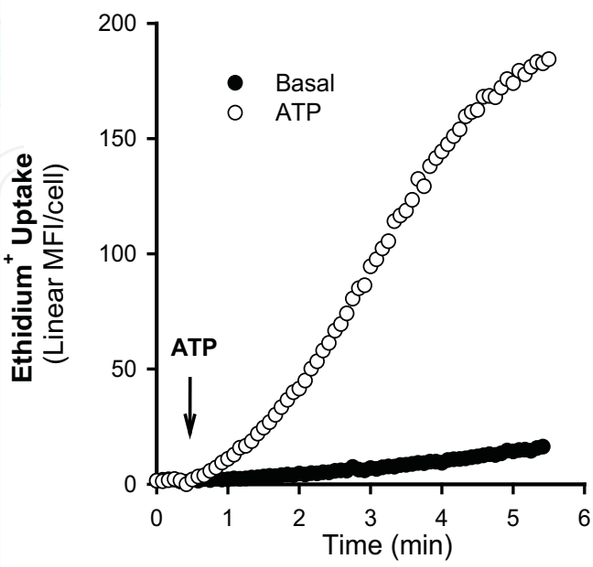

Fig. 7. An example of spreadsheet (left) and a typical curve of ethidium$^+$ uptake (right)

Function(D6)
=2.5*(SUM(INDIRECT(ADDRESS(D4+8,COLUMN(),4,1),1):INDIRECT(ADDRESS(D4+5*12+8,COLUMN(),4,1),1))+SUM(INDIRECT(ADDRESS(D4+9,COLUMN(),4,1),1):INDIRECT(ADDRESS(D4+5*12+7,COLUMN(),4,1),1))-SUM(INDIRECT(ADDRESS(D4+8,COLUMN()-1,4,1),1):INDIRECT(ADDRESS(D4+5*12+8,COLUMN()-1,4,1),1))-SUM(INDIRECT(ADDRESS(E4+9,COLUMN()-1,4,1),1):INDIRECT(ADDRESS(D4+5*12+7,COLUMN()-1,4,1),1))-(D5-C5)*120)
(to calculate uptake curve in the first 5 min after area under ethidium$^+$ uptake curve after addition of ATP)

The arbitrary unit obtained in Function(D6) is used to quantify the P2X7 pore function. Time frame chosen for calculation of ATP-induced ethidium$^+$ uptake is 5 min. This is simply because the linear response after addition of ATP is about 5 min. However, in monocytes from some healthy subjects with high P2X7 function, ATP may induce a linear response only in the first 2 or 3 min before the fluorescence of cell-associated ethidium reaches the maximum channel number. The calculation model can be readily adapted to shorter time points on the ethidium$^+$ uptake curve. To do this, the time point in above function (5*) can be replaced by 2*, 3* or 4* for 2, 3 or 4 min respectively.

3.4 Notes for technique

The peak channel of Standard PE Reference Beads measured on linear mode in FL2 can be as large as ±20% from one day to another. Therefore it is essential to calibrate the instrument daily before each set of experiments. Furthermore, ethidium$^+$ concentration, temperature and the composition of the suspending buffer are critical parameters. The area under the ethidium$^+$ uptake curve increases proportionally with the ethidium$^+$ concentration up to about 100 μM. Excess ethidium$^+$ however might bind to mitochondrial membranes and lead to inaccurate results. Moreover, P2X7 function is dependent on temperature. We have shown that P2X7 agonists fail to induce ethidium$^+$ uptake at 12^{o}C, which is gradually restored by a temperature rise up to a physiological value of 37^{o}C. Results are further altered by the absence or presence of Ca^{2+}, Cl^- and Na^+ ions in the acquisition medium. Small amounts of extracellular Ca^{2+} (~10 μM) in the medium are always included to maintain cell membrane integrity. However, high concentration of Ca^{2+} may reduce the ATP activity by binding to its active species, ATP^{4-} or by direct competition for permeation (Wiley *et al.*, 1996). Isotonic K^+ or sucrose media remove the inhibitory effect of Na^+ and/or Cl^- ions on P2X7 function, which facilitates the detection of differences in P2X7 function among individuals. Since multiple factors cause large alterations in the area under the ethidium uptake curve, it is essential to keep standardized assay conditions.

ATP-induced ethidium$^+$ uptake is directly proportional to the concentration of ethidium cation over the range 1 to 100 μM, consistent with permeation of ethidium$^+$ through a dilated pore. 25 μM ethidium bromide is routinely used for measurement of uptakes over a 3 to 5 minute time course. The pore formation by activated P2X7 is also sensitive to temperature. P2X7 function decreases at lower temperature while at 12^{o}C or lower, ATP-induced ethidium$^+$ uptake is almost completely abolished. It has been reported that removal of extracellular Cl^- as well as extracellular Na^+ enhances permeability responses and stimulates the function of the P2X7 receptor (Michel *et al.*, 1999). P2X7 function measured by ATP-induced ethidium$^+$ uptake is greatest in Na^+ free, Cl^- free sucrose medium, less in KCl medium, and least in NaCl medium.

Leukocyte subtypes are identified by monoclonal antibodies and we observed that unconjugated anti-CD14, CD3, CD19 or CD16 antibody did not affect ATP-induced ethidium$^+$ uptake. Thus, with the correct FL2-FL1 compensation, the positively gated population should give a similar value of area under ethidium$^+$ uptake curve as the negatively gated population. While the extremely bright fluorescence of ethidium$^+$ makes for accuracy in the uptake measurement, it does make the correct compensation between FL1 and FL2 essential. While under-compensation of FL2-FL1 leads to high basal level of ethidium$^+$ uptake, any over-compensation of FL2-FL1 dramatically reduces the area under ethidium$^+$ uptake curves. Meanwhile, if the FL1-FL2 compensation is too high or too low, the R2 gated population (Fig. 6) will incline towards left or right, respectively. Ethidium$^+$ uptake can also exclude the necrotic or apoptotic cells from the live cells in the suspension, simply by excluding fluorescent events at the maximum fluorescent channel intensity at zero time which defines the fully permeabilized cells present.

4. Phagocytosis of fluorescent latex beads

4.1 Introduction

Phagocytosis is a fundamental aspect of the innate immune system which is preserved in specialized cells of all metazoans. Human monocytes suspended in saline media (without serum) rapidly phagocytose a range of foreign particles which are internalized into a phagosome via rearrangement of the actin-myosin cytoskeleton. This innate immune function requires recognition of foreign particles by one or more scavenger receptors on the monocyte surface. We have recently shown that an intact P2X7-nonmuscle myosin heavy chain IIA complex in monocyte/macrophages can regulate the phagocytosis of a range of non-opsonized particles including latex beads, and live and dead *Staphylococcus aureus* and *Escherichia coli* (Gu *et al*., 2010).

Technical advances in the assessment of phagocytosis have allowed rapid advances in our knowledge of molecular interactions associated with engulfment of particles by phagocytes. Confocal microscopy has shown that internal membranes within the cell fuse with plasma membrane during the course of particle ingestion, and that recycling endosomes are the primary source of membrane for enlargement of phagocytic cup (Touret *et al*., 2005). Flow cytometric assessment of particle engulfment has to some extent replaced microscopic observation (Steinkamp *et al*., 1982) particularly as the kinetics of uptake of fluorescent targets by phagocytes can be followed by instruments capable of time-resolved measurements in a stirred cuvette at 37^{o}C (Gu *et al*., 2010). These assays of phagocytosis by flow cytometry usually include measurements of fluorescence particle uptake by cells pre-incubated with cytochalasin D (CytD), an inhibitor of F-actin polymerization and phagocytic cup formation and this control condition allows the assay to distinguish engulfment of particles from adhesion. Particle size is also important in flow studies which generally employ fluorescent particles ranging from 1 to 3 μm in diameter.

Various methods have been employed in phagocytosis studies. However, no published method reflects the quantitative particle uptake in real time although this parameter is important to fully assess the engulfment ability of phagocytes. In this section, we describe a quantitative method to measure the phagocytic ability of human monocytes using time-resolved two-colour flow cytometry.

4.2 Method

Mononuclear cells (2×10^6 in 100 µL) are pre-labeled with APC conjugated-anti CD14 followed by addition of 900 µL Na medium with 0.1 mM Ca^{2+} with a small magnetic stir bar. The tube is inserted into the Time-Zero System (from Cytek Development, Fremont, CA, USA) which monitors temperature (37°C) and allows magnetic stirring. 5 to 10 µL yellow-green carboxylated fluorescent polystyrene latex microspheres (YG bead, 1 µm, from Polyscience, Warrington, PA) are added 20 sec later. Linear MFI of YG fluorescence is collected in FL1 (voltage: 380-420, gain: 2.0). Events are acquired at about 1500 events per second by a Becton Dickinson FACSCalibur flow cytometer. The data of each run are collected for about 7 min and saved into a listmode file.

4.3 Gating and calculation

The listmode file is analysed by WinMDI. Cells are gated by forward and side scatter and by cell type specific antibodies (Fig. 8). The linear mean channel of fluorescence intensity for each gated subpopulation over successive 10 sec intervals is plotted against time to yield kinetic data which is saved into a text file.

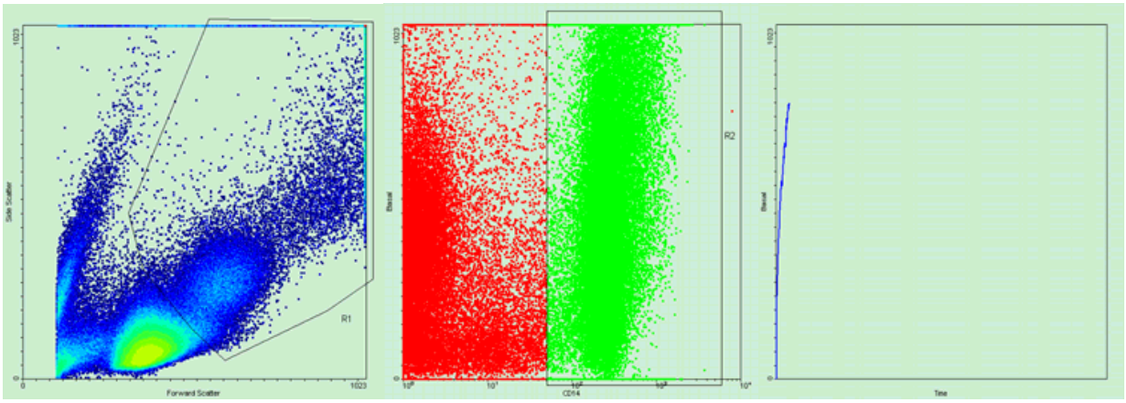

Fig. 8. Typical dotplots and gating strategy used to analyse YG bead uptake by $CD14^+$ monocytes

To quantify bead uptake, arbitrary units of area under the uptake curve in first 6.5 min after addition of beads is calculated. The area is considered as the sum of 39 trapezoids, which is calculated by the following mathematical model. The text file is then imported into *Microsoft* Excel, and mathematical calculation of the area under the bead uptake curve is programmed using the following functions:

C5, D5 and E5 are the lowest value among C6, D6 and E6, represent the threshold to exclude the background fluorescence intensity.

Function(C6)=INDIRECT(ADDRESS(MATCH(30,C$9:C$32,1)+10,COLUMN(),4,1),1)
(To calculate initial levels of fluorescence intensity)

Function(C7)=5*(C$6+2*SUM(INDIRECT(ADDRESS(MATCH(30,C$9:C$32,1)+11,COLUMN(),4,1),1):INDIRECT(ADDRESS(MATCH(30,C$9:C$32,1)+6.5*6+9,COLUMN(),4,1),1))+INDIRECT(ADDRESS(MATCH(30,C$9:C$32,1)+6.5*6+10,COLUMN(),4,1),1))-C$6*6.5*6*10
(To calculate area under YG bead uptake curve in the first 6.5 min)

The area under the YG bead uptake curve is calculated over the time frame of 6.5 min, because the uptake of beads is usually maximal at this time point. However, the calculation model can be readily adapted to different time points on the YG bead uptake curve. To do this, the time point in above function (ie 6.5) can be replaced by the desired time in minutes.

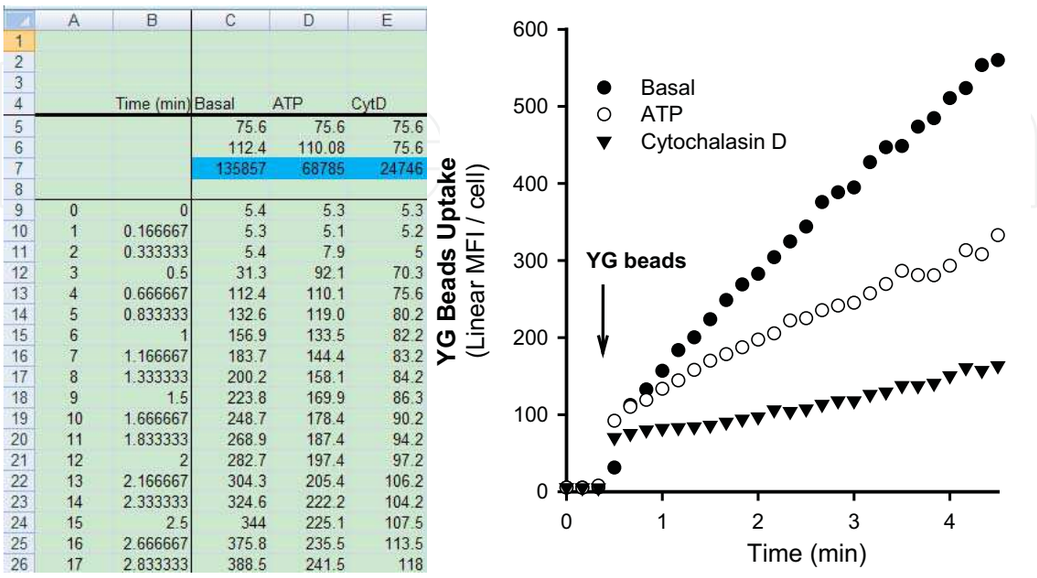

	A	B	C	D	E
1					
2					
3					
4		Time (min)	Basal	ATP	CytD
5			75.6	75.6	75.6
6			112.4	110.08	75.6
7			135857	68785	24746
8					
9	0	0	5.4	5.3	5.3
10	1	0.166667	5.3	5.1	5.2
11	2	0.333333	5.4	7.9	5
12	3	0.5	31.3	92.1	70.3
13	4	0.666667	112.4	110.1	75.6
14	5	0.833333	132.6	119.0	80.2
15	6	1	156.9	133.5	82.2
16	7	1.166667	183.7	144.4	83.2
17	8	1.333333	200.2	158.1	84.2
18	9	1.5	223.8	169.9	86.3
19	10	1.666667	248.7	178.4	90.2
20	11	1.833333	268.9	187.4	94.2
21	12	2	282.7	197.4	97.2
22	13	2.166667	304.3	205.4	106.2
23	14	2.333333	324.6	222.2	104.2
24	15	2.5	344	225.1	107.5
25	16	2.666667	375.8	235.5	113.5
26	17	2.833333	388.5	241.5	118

Fig. 9. An example of spreadsheet (left) and a typical curve of YG bead uptake (right)

4.4 Notes for technique

The time resolved flow cytometry based method described here allows real-time quantitative assessment of the phagocytic function of peripheral blood monocytes labeled with APC conjugated CD14 antibody. The excitation and emission wavelength of APC is well separated from the YG-beads containing fluorescein (APC: Ex. 633nm, Em. 660nm; YG: Ex. 441nm, Em. 486nm), thus the compensation setting of the flow cytometer can be ignored. Although lymphocytes do not phagocytose 1 µm YG bead in this setting (Gu *et al.*, 2010), the $CD14^+$ gating is necessary to exclude uptake of YG beads by the small number of neutrophils which contaminate the Ficoll separated mononuclear population.

Since the bead size is much less than cell size, multiple beads transit through the laser beam together with the cell, leading to a considerable fluorescence background. In addition, some YG beads may also adhere to cell surface non-specifically. Thus cytochalasin D (a potent phagocytosis inhibitor) is used to assess fluorescence intensity due to background resulting from above factors.

Many factors can affect this phagocytosis assay including the nature of bead surface. The total uptake of negatively charged carboxylate beads is higher than the uptake of uncharged beads suggesting the negatively charged carboxyl groups on the bead surface facilitates their uptake by monocytes. The bead size, cell:bead ratio, pH and temperature are critical parameters affecting uptake. Uptake of 1 µm beads is maximal at a pH 6.5-7.5 and 37°C in serum-free Na medium with 0.1 mM Ca^{2+}. This method can be used to compare the phagocytic ability of monocytes from different individuals, especially if a standard protocol is used and the flow cytometer is carefully calibrated from day-to-day.

5. Protein complex dissociation

5.1 Principle

Fluorescence resonance energy transfer (FRET) is one of the major techniques used for protein interaction studies. Confocal or fluorescent microscopes with photobleach or fluorescence lifetime modules are the common instruments which perform FRET based measurements. However, microscopy can only detect fluorescence signals in a single cell, and cannot measure multiple fluorescence emission wavelengths simultaneously. This limitation on confocal microscope makes flow cytometer an attractive alternative for FRET based measurement. The time-resolved fluorescence decay measurement by flow cytometry has been used to study molecule interactions (Condrau *et al*., 1994a; Condrau *et al*., 1994b; Deka & Steinkamp, 1996). However, this technique requires major modification to a flow cytometer since a pulsed laser has to be used in order to measure fluorescence lifetime.

The P2X7 receptor has been shown to form a protein complex with nonmuscle myosin heavy chain IIA (NMMHC-IIA) in its unactivated state, and this complex dissociates following activation of P2X7 by extracellular ATP (Gu *et al*., 2009). To study the interaction of these two proteins in a large cohort of live cells, we developed a time-resolved FRET (TR-FRET) flow cytometry method. The HEK-293 cells are transfected with AcGFP-tagged NMMHC-IIA and DsRed-tagged P2X7. The NMMHC-P2X7 interaction is assessed by monitoring the fluorescence intensity changes of AcGFP and DsRed in double positive cells over 10-15 minutes after addition of P2X7 agonist. This method does not require any modification of the flow cytometer, and can be readily adapted to study the interaction within the intact cell of virtually any two tagged proteins expressed in a large cohort of transfected live cells.

5.2 Method

HEK-293 cells co-transfected with *pAcGFP-N1-MYH9* (the gene encoding NMMHC-IIA) and *pDsRed-monomer-N1-P2RX7* (1:4) are resuspended in Na medium with 0.1 mM $CaCl_2$ at a concentration of $2.0x10^6$/mL. The cell suspension (2 mL) is stirred and temperature maintained at 37°C using a Time Zero module. ATP (1.0 mM) is added 2 min after the tube is inserted. Cells are analysed at about 1500 events/s on a FACSCalibur flow cytometer. The voltage settings and compensation are established using non-transfected cell and cells transfected with either AcGFP or DsRed. The FSC, SSC, log FL1, log FL3 and the time are collected into a FCS 2.0 file.

5.3 Gating and calculation

Fluorescent events are gated by forward and side scatter and by AcGFP and DsRed fluorescence intensity. The log mean channel of fluorescence intensity for each gated subpopulation over successive 5-s intervals is analysed by WinMDI software and saved into a text file.

To quantify levels of protein dissociation, arbitrary unit of area under/above the kinetic fluorescence curve in first 12 min after addition of ATP is calculated. The text file is then imported into *Microsoft* Excel spreadsheet, and mathematical calculation of the area under/above curve is programmed using the following functions:

Function(C4)=MATCH(0,C$7:C$40,0) ; *To calculate when ATP is added.*

Function (C5)=AVERAGE(C$7:INDIRECT(ADDRESS(C$4+5,COLUMN(),4,1),1))
To calculate the base line.

Function(C6)
=0.5*5*(INDIRECT(ADDRESS(C$4+7,COLUMN(),4,1),1)+2*SUM(INDIRECT(ADDRESS(C$4+8,COLUMN(),4,1),1):INDIRECT(ADDRESS(C$4+12*12+6,COLUMN(),4,1),1))+INDIRECT(ADDRESS(C$4+12*12+7,COLUMN(),4,1),1))-C$5*12*12*5
To calculate area above/under curve (Log mode)

Funciton(D7)=IF(C7=0,0,POWER(10,(C7+1)/256))
To transform the log MFI to artificial linear MFI. The rest data in Column D are transformed using the same function by "Ctrl-D" command.

Function(D6)
=0.5*5*(INDIRECT(ADDRESS(D$4+7,COLUMN(),4,1),1)+2*SUM(INDIRECT(ADDRESS(D$4+8,COLUMN(),4,1),1):INDIRECT(ADDRESS(D$4+12*12+6,COLUMN(),4,1),1))+INDIRECT(ADDRESS(D$4+12*12+7,COLUMN(),4,1),1))-D$5*12*12*5
To calculate area above/under curve (Linear mode)

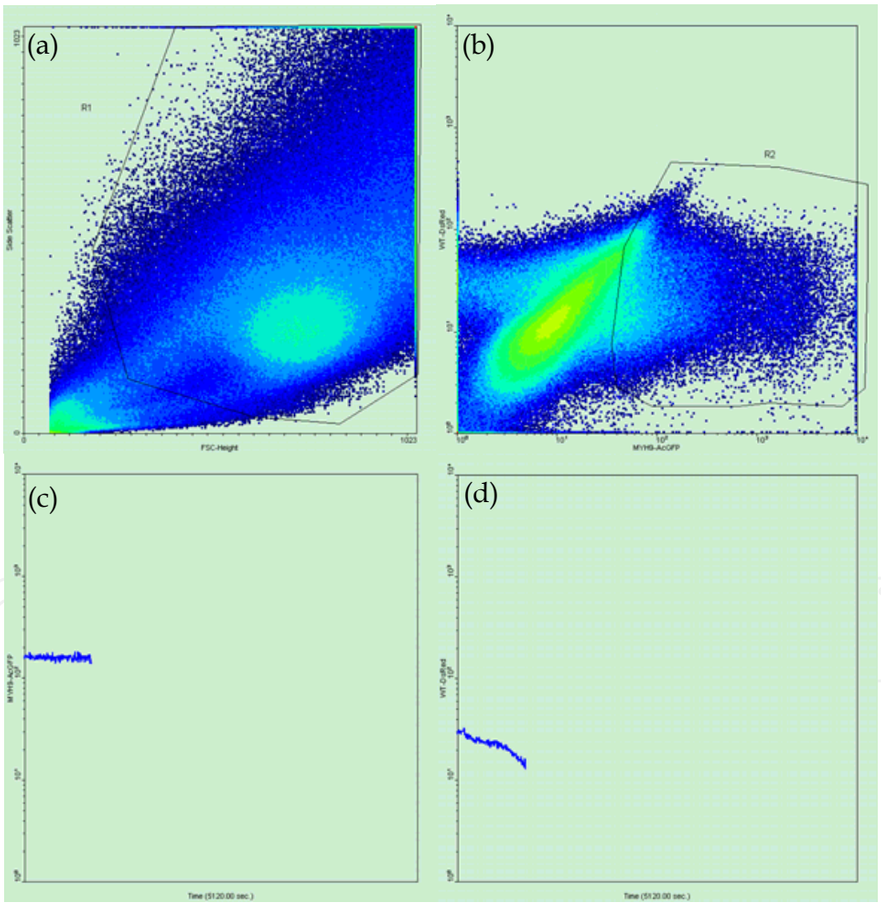

Fig. 10. Typical dotplots and gating strategy used to analyse protein-protein interaction. **a.** The FSC and SSC of HEK-293 cells gated by gate R1. **b.** The AcGFP$^+$DsRed$^+$ HEK-293 cells gated by R2. **c.** Changes in fluorescence of AcGFP tagged NMMHC-IIA. **d.** Kinetic P2X7 with time of DsRed tagged fluorescence

	A	B	C	D	E	F
1						
2		Time (min)	Wild Type P2X7 with BzATP			
3			AcGFP		DsRed	
4			18	18	18	18
5			605.71	234.78	400.21	36.95
6			9455	21248	-27681	-6960
7	0	0	594.8	212.4926	406	38.8905
8	1	0.083333	602.9	228.5517	407.4	39.3833
9	2	0.166667	612.7	249.6121	399.5	36.682
10	3	0.25	601.7	226.0981	400.3	36.9469
11	4	0.333333	618.7	263.453	402.9	37.8211
12	5	0.416667	606.4	235.8611	398.1	36.223
13	6	0.5	604.6	232.0732	402.3	37.6176
14	7	0.583333	599.2	221.0707	406.3	38.9956
15	8	0.666667	601.4	225.4888	400	36.8473
16	9	0.75	614.3	253.2303	403	37.8552
17	10	0.833333	605.5	233.9595	403.2	37.9233
18	11	0.916667	611.7	247.377	399.1	36.5503
19	12	1	613.7	251.8674	398	36.1904
20	13	1.083333	601.1	224.8812	398.8	36.4518
21	14	1.166667	598.7	220.0788	392.8	34.5367
22	15	1.25	606.2	235.4372	393.3	34.6924
23	16	1.333333	603.5	229.7884	392.6	34.4747
24	17	1.416667	0	0	0	0
25	18	1.5	596	214.7985	397.3	35.9633
26	19	1.583333	610.5	244.7214	392.7	34.5057
27	20	1.666667	608.7	240.7912	398	36.1904
28	21	1.75	600.2	223.0681	391.1	34.0127

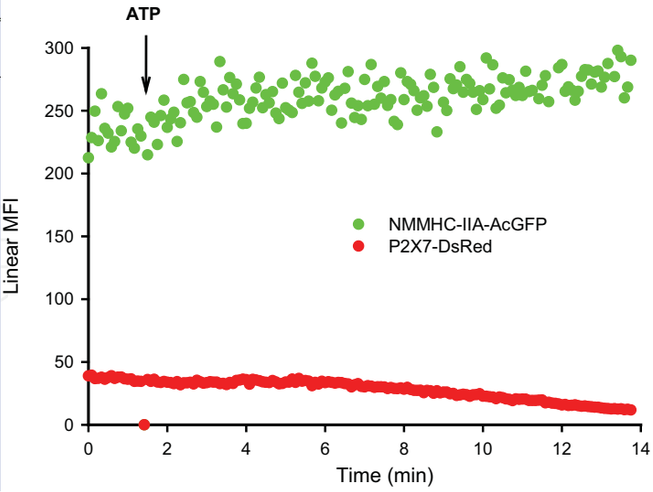

Fig. 11. An example of spreadsheet (left) and a typical curve of protein dissociation (right)

5.4 Notes for technique

The compensation setting in this application is critical. HEK-293 transfected with either AcGFP- or DsRed-tagged protein should be used to establish correct compensation. Although data on FL2 is not collected, the voltage should still be set at a similar level to FL1 to enable compensation between FL1 and FL3.

AcGFP and DsRed is a good pair of FRET partners for flow cytometry. Both AcGFP and DsRed are monomers, thus possible self-polymerization can be avoided. A regular 488 laser is optimized to excite AcGFP fluorescence signal but has gives little excitation of DsRed. The emission wavelength of AcGFP is in the optimum range for excitation of DsRed. Therefore, the DsRed emission signal is mainly due to the FRET effect. With careful compensation settings, the AcGFP and DsRed emissions can be readily studied in a real time flow cytometry system using only a 488nm laser. This method allows a quick and reliable assessment of protein dissociation. The dissociation rate can be compared between samples in the same experiment. However, this method cannot provide an estimated value for FRET efficiency derived according to Förster formulae (Förster, 1948).

6. Discussion

Although flow cytometry is a mature technique and time-resolved flow cytometry (TR-FCM) has been widely used in cellular kinetic study, the great potential of TR-FCM has not been fully realized by most researchers. In part this is due to the requirement of modification of existing instruments as well as data analysis. The four applications described in this chapter are simple and feasible, requiring only minimum modification of the flow cytometer. The Time-Zero module can be easily set up in less than 5 min. If this module is not available, a small beaker with 37°C water can substitute for temperature control. The analysis software is free and the example of MS Excel templates are available. We hope above four examples may encourage the use of TR-FCM in more cellular kinetic studies.

The new generation of flow cytometers, such as Accuri C6 from BD, MACSQuant Analyzer from Miltenyi Biotec, Cyan from Beckman Coulter, Attune Acoustic Focusing Cytometer from Invitrogen, uses "plugs" to deliver sample for analysis (Edwards *et al.*, 2001a). This analyses precise defined volume and the sample vessel need not be pressurized. However, none of these cytometers can perform TR-FCM applications described in this chapter, although all have the time parameter for acquisition. Manufacturers have not realized the importance of TR-FCM, and its marketing value. In fact, with small modification of the sample platform and the acquisition software, these new generation of flow cytometers can easily be upgraded for TR-FCM.

7. References

Condrau, M.A., Schwendener, R.A., Niederer, P. & Anliker, M. (1994a). Time-resolved flow cytometry for the measurement of lanthanide chelate fluorescence: I. Concept and theoretical evaluation. *Cytometry*,Vol. 16,No.3, pp.187-94

Condrau, M.A., Schwendener, R.A., Zimmermann, M., Muser, M.H., Graf, U., Niederer, P. & Anliker, M. (1994b). Time-resolved flow cytometry for the measurement of lanthanide chelate fluorescence: II. Instrument design and experimental results. *Cytometry*,Vol. 16,No.3, pp.195-205

Deka, C. & Steinkamp, J.A. (1996). Time-resolved fluorescence-decay measurement and analysis on single cells by flow cytometry. *Appl Opt*,Vol. 35,No.22, pp.4481-9

Edwards, B.S., Kuckuck, F.W., Prossnitz, E.R., Okun, A., Ransom, J.T. & Sklar, L.A. (2001a). Plug flow cytometry extends analytical capabilities in cell adhesion and receptor pharmacology. *Cytometry*,Vol. 43,No.3, pp.211-6

Edwards, B.S., Kuckuck, F.W., Prossnitz, E.R., Ransom, J.T. & Sklar, L.A. (2001b). HTPS flow cytometry: a novel platform for automated high throughput drug discovery and characterization. *Journal of biomolecular screening*,Vol. 6,No.2, pp.83-90

Förster, T. (1948). Intermolecular energy migration and fluorescence. *Annalen der Physik*,Vol. 437,No.2, pp.55-75

Gomperts, B.D. (1983). Involvement of guanine nucleotide-binding protein in the gating of Ca2+ by receptors. *Nature*,Vol. 306,No.5938, pp.64-6

Gu, B.J., Rathsam, C., Stokes, L., McGeachie, A.B. & Wiley, J.S. (2009). Extracellular ATP dissociates nonmuscle myosin from P2X7 complex: this dissociation regulates P2X7 pore formation. *Am J Physiol Cell Physiol*,Vol. 297,No.2, pp.C430-439

Gu, B.J., Saunders, B.M., Jursik, C. & Wiley, J.S. (2010). The P2X7-nonmuscle myosin membrane complex regulates phagocytosis of non-opsonized particles and bacteria by a pathway attenuated by extracellular ATP. *Blood*,Vol. 115,No.8, pp.1621-1631

Gu, B.J., Saunders, B.M., Petrou, S. & Wiley, J.S. (2011). P2X7 is a scavenger receptor for apoptotic cells in the absence of its ligand extracellular ATP. *Journal of Immunology*,Vol. 187,No.5, pp.2365-2375

Gu, B.J., Sluyter, R., Skarratt, K.K., Shemon, A.N., Dao-Ung, L.P., Fuller, S.J., Barden, J.A., Clarke, A.L., Petrou, S. & Wiley, J.S. (2004). An Arg307 to Gln polymorphism within the ATP-binding site causes loss of function of the human P2X7 receptor. *Journal of Biological Chemistry*,Vol. 279,No.30, pp.31287-95

Gu, B.J., Zhang, W., Worthington, R.A., Sluyter, R., Dao-Ung, P., Petrou, S., Barden, J.A. & Wiley, J.S. (2001). A Glu-496 to Ala polymorphism leads to loss of function of the human P2X7 receptor. *Journal of Biological Chemistry*,Vol. 276,No.14, pp.11135-42

Gu, B.J., Zhang, W.Y., Bendall, L.J., Chessell, I.P., Buell, G.N. & Wiley, J.S. (2000). Expression of P2X7 purinoceptors on human lymphocytes and monocytes: evidence for

nonfunctional P2X7 receptors. *American Journal of Physiology - Cell Physiology*,Vol. 279,No.4, pp.C1189-97

Humphreys, B.D. & Dubyak, G.R. (1996). Induction of the P2Z/P2X7 nucleotide receptor and associated phospholipase D activity by lipopolysaccharide and IFN-gamma in the human THP-1 monocytic cell line. *Journal of Immunology*,Vol. 157,No.12, pp.5627-37

Jursik, C., Sluyter, R., Georgiou, J.G., Fuller, S.J., Wiley, J.S. & Gu, B.J. (2007). A quantitative method for routine measurement of cell surface P2X(7) receptor function in leucocyte subsets by two-colour time-resolved flow cytometry. *J Immunol Methods*,Vol. 32567-77

Michel, A.D., Chessell, I.P. & Humphrey, P.P. (1999). Ionic effects on human recombinant P2X7 receptor function. *Naunyn-Schmiedebergs Archives of Pharmacology*,Vol. 359,No.2, pp.102-9

Nolan, J.P. & Sklar, L.A. (1998). The emergence of flow cytometry for sensitive, real-time measurements of molecular interactions. *Nature Biotechnology*,Vol. 16,No.7, pp.633-8

Ramirez, S., Aiken, C.T., Andrzejewski, B., Sklar, L.A. & Edwards, B.S. (2003). High-throughput flow cytometry: validation in microvolume bioassays. *Cytometry Part A: the journal of the International Society for Analytical Cytology*,Vol. 53,No.1, pp.55-65

Shemon, A.N., Sluyter, R., Fernando, S.L., Clarke, A.L., Dao-Ung, L.P., Skarratt, K.K., Saunders, B.M., Tan, K.S., Gu, B.J., Fuller, S.J., Britton, W.J., Petrou, S. & Wiley, J.S. (2006). A Thr(357) to Ser polymorphism in homozygous and compound heterozygous subjects causes absent or reduced P2X(7) function and impairs ATP-induced mycobacterial killing by macrophages. *Journal Of Biological Chemistry*,Vol. 281,No.4, pp.2079

Skarratt, K.K., Fuller, S.J., Sluyter, R., Dao-Ung, L.P., Gu, B.J. & Wiley, J.S. (2005). A 5 ' intronic splice site polymorphism leads to a null allele of the P2X(7) gene in 1-2% of the Caucasian population. *Febs Letters*,Vol. 579,No.12, pp.2675

Sklar, L.A., Carter, M.B. & Edwards, B.S. (2007). Flow cytometry for drug discovery, receptor pharmacology and high-throughput screening. *Curr Opin Pharmacol*,Vol. 7,No.5, pp.527-34

Steinkamp, J.A., Wilson, J.S., Saunders, G.C. & Stewart, C.C. (1982). Phagocytosis: flow cytometric quantitation with fluorescent microspheres. *Science*,Vol. 215,No.4528, pp.64-6

Touret, N., Paroutis, P., Terebiznik, M., Harrison, R.E., Trombetta, S., Pypaert, M., Chow, A., Jiang, A., Shaw, J., Yip, C., Moore, H.P., van der Wel, N., Houben, D., Peters, P.J., de Chastellier, C., Mellman, I. & Grinstein, S. (2005). Quantitative and dynamic assessment of the contribution of the ER to phagosome formation. *Cell*,Vol. 123,No.1, pp.157-70

Wiley, J.S., Chen, J.R., Snook, M.S., Gargett, C.E. & Jamieson, G.P. (1996). Transduction mechanisms of P2Z purinoceptors. *Ciba Foundation Symposium*,Vol. 198149-60; discussion 160-5

Wiley, J.S., Chen, R., Wiley, M.J. & Jamieson, G.P. (1992). The ATP4- receptor-operated ion channel of human lymphocytes: inhibition of ion fluxes by amiloride analogs and by extracellular sodium ions. *Archives of Biochemistry & Biophysics*,Vol. 292,No.2, pp.411-8

Wiley, J.S., Dao-Ung, L.-P., Li, C., Shemon, A.N., Gu, B.J., Smart, M.L., Fuller, S.J., Barden, J.A., Petrou, S. & Sluyter, R. (2003). An Ile-568 to Asn Polymorphism Prevents Normal Trafficking and Function of the Human P2X7 Receptor. *Journal of Biological Chemistry*,Vol. 278,No.19, pp.17108-17113

Wiley, J.S., Gargett, C.E., Zhang, W., Snook, M.B. & Jamieson, G.A. (1998). Partial agonists and antagonists reveal a second permeability state of human lymphocyte P2Z/P2X7 channel. *American Journal of Physiology - Cell Physiology*,Vol. 44,No.5, pp.C1224-C1231

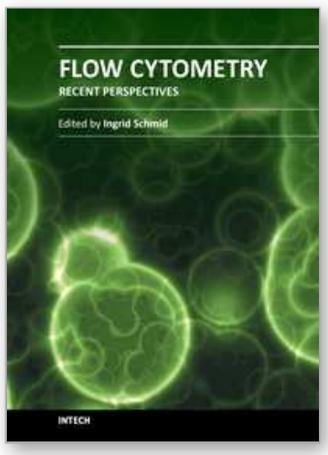

Flow Cytometry - Recent Perspectives

Edited by M.Sc. Ingrid Schmid

ISBN 978-953-51-0626-5
Hard cover, 500 pages
Publisher InTech
Published online 13, June, 2012
Published in print edition June, 2012

"Flow Cytometry - Recent Perspectives" is a compendium of comprehensive reviews and original scientific papers. The contents illustrate the constantly evolving application of flow cytometry to a multitude of scientific fields and technologies as well as its broad use as demonstrated by the international composition of the contributing author group. The book focuses on the utilization of the technology in basic sciences and covers such diverse areas as marine and plant biology, microbiology, immunology, and biotechnology. It is hoped that it will give novices a valuable introduction to the field, but will also provide experienced flow cytometrists with novel insights and a better understanding of the subject.

InTech Europe
University Campus STeP Ri
Slavka Krautzeka 83/A
51000 Rijeka, Croatia
Phone: +385 (51) 770 447
Fax: +385 (51) 686 166
www.intechopen.com

InTech China
Unit 405, Office Block, Hotel Equatorial Shanghai
No.65, Yan An Road (West), Shanghai, 200040, China
中国上海市延安西路65号上海国际贵都大饭店办公楼405单元
Phone: +86-21-62489820
Fax: +86-21-62489821

IntechOpen